World Journal of Pharmaceutical research

Volume 3, Issue 2, 3066-3092. Research Article ISSN 2277 – 7105

TRANSDERMAL DELIVERY OF STAVUDINE USING PENETRATION ENHANCERS

Jai Deo Pandey[1], Ritu Singh[*1] and Nripendra Singh[2]

[1]Dept.of Pharmaceutics, R.R.S college of pharmacy, Amethi, Sultanpur, U.P., India.

[2]Dept. of Pharmacy, V.B.S. Purvanchal University, Jaunpur, India.

Article Received on
05 January 2014,

Revised on 25 January 2014,
Accepted on 27 February 2014

***Correspondence for Author**
Ritu Singh
Dept.of Pharmaceutics, R.R.S college of pharmacy, Amethi, Sultanpur, U.P., India.

ABSTRACT

The purpose of this research work was formulation and evaluation of transdermal drug delivery system of Stavudine using suitable penetration enhancers by using solvent evaporation technique for improvement of bioavailability of drug and reducing toxic effects. Chitosan membranes were obtained by a casting/solvent method and cross-linking with sodium tripolyphosphate. The prepared formulations were evaluated for various parameters like weight, thickness, drug content, percentage moisture content, percentage moisture uptake, tensile strength, folding endurance, *In vitro* drug release and *in vitro* permeation studies. Also these patches were characterized by Scanning Electron Microscopy, Fourier transforms Infrared Spectrosphotometry, Differential Scanning Calorimeter, X-ray diffraction, skin irritation and stability. All the patches were uniform with respect to physicochemical evaluation. FTIR study and DSC analysis showed that there was no significant interaction between the drug and polymers. X-ray diffraction study indicating that drug in the matrix film is not present completely in the crystalline state, but is in the amorphous solid dispersion state. The result of diffusion study shows that formulation F10 (oleic acid) showed maximum diffusion of 89.35% in 10 h, whereas F6 (without enhancer) showed minimum diffusion of 24.81% in 10 h.The various permeation parameters were determined for all the formulations. The maximum flux was obtained with F10 formulation. All the films were found to be stable with respect to their physical parameters and drug content. Drug release kinetics has shown that formulations F6 and F10 follow first order kinetics. The n values obtained between 0.878 to 1.131 which indicates that the release approximates non fickian diffusion and case II transport. It was concluded that the results of drug permeation from transdermal patches (F10 and F9) of stavudine through excised rat

abdominal skin confirmed that Stavudine was released from the formulation and permeated through the rat skin and hence could possibly permeate through the human skin.

Key words: Stavudine, Chitosan, Penetration enhancers, *In*- vitro evaluation.

INTRODUCTION

Viral disease is one of the most prevalent diseases in the modern world. Many viruses eventually kill their host cells, resulting in disease and provoking an assault by the immune response of the host (1). The worldwide viral diseases are Acquired immunodeficiency syndrome (AIDS), Dengue, Encephalitis, Hepatitis, Yellow fever (2). Approximately million people are suffering from AIDS worldwide. This highlights the importance of treating AIDS (3). It is characterized by gradual destruction of cell-mediated (T-cell) immunity; it also affects humoral immunity and autoimmunity because of the central role of the $CD4^+$ T lymphocyte in immune reactions (4). Nucleoside reverse transcriptase inhibitors (NRTIs) are the first class of antiretrovirals. Stavudine (D4T) is one of the most essential NRTIs for AIDS treatment that is active *in vitro* against HIV-1 and HIV-2 (5). It is absorbed rapidly following oral administration producing peak plasma concentration within 1 hour with 86 % bioavailability. Elimination half-life is 1 to 1.5 hours following single or multiple doses. In addition to pharmacokinetic properties, stavudine has low dose, low molecular weight (224.2) and extensive first pass effect (6). All the above properties are reflecting on its suitability and necessity as a good candidate for transdermal delivery. A Recent approach to drug delivery is to deliver the drug into systemic circulation at predetermined rate using skin as a site of application. Transdermal patches are delivered the drug through the skin in controlled and predetermined manner in order to increase the therapeutic efficacy of drug and reduced side effect of drug (7). Controlled drug release can be achieved by transdermal drug delivery systems (TDDS) which can deliver medicines via the skin portal to systemic circulation at a predetermined rate over a prolonged period of time. TDDS has gained a lot of interest during the last decade as it offers many advantages over the conventional dosage forms and oral controlled release delivery systems notably avoidance of hepatic first pass metabolism, less frequency of administration, reduction in gastrointestinal side effects and improves patient compliance (8). Chitosan, a natural, biodegradable, biocompatible, bioadhesive polymer, is gaining attention in the pharmaceutical field for a wide range of drug delivery. Chitosan is a copolymer of glucosamine and N-acetyl glucosamine linked by β 1–4 glucosidic bonds obtained by N-deacetylation of chitin (9). The molecular weight and degree of deacetylation

can be modified during its preparation to obtain tailor-made properties. Also, chitosan has free amine as well as hydroxyl groups, which can be modified to obtain different chitosan derivatives (10). Chitosan acts as a penetration enhancer by opening the tight epithelial junctions (11). Chitosan being cationic in nature offers great advantages for ionic interactions. Chitosan is polycationic in acidic media (pKa 6.5) and can interact with negatively charged species such as TPP (12, 13). This characteristic can be employed to prepare cross-linked chitosan membrane. The interaction of chitosan with TPP leads to formation of biocompatible cross-linked chitosan membrane, which can be efficiently employed in drug delivery (14). The cross-linking density, crystallinity, and hydrophilicity of cross-linked chitosan can allow modulation of drug release and extend its range of potential applications in drug delivery (15, 16). It was found that terpenes and fatty acids at 5% w/v in vehicle were effective in achieving permeation rates that were sufficient to show a therapeutic effect. Terpenes, naturally occuring volatile oils, appear to be promising candidates for clinically acceptable enhancers (17). Terpenes are generally considered as less toxic and have less irritant effects compared to surfactants and other skin penetration enhancers, and some terpenes have been characterized as Generally Recognized As Safe (GRAS) by the US FDA. They have high percutaneous enhancement ability, reversible effect on the lipids of stratum corneum, and minimal percutaneous irritancy at low concentrations (1-5%) (18). Moreover, a variety of terpenes have been shown to increase percutaneous absorption of both hydrophilic and lipophilic drugs (19, 20).

The objective of the present work was to develop and characterize the stavudine transdermal therapeutic systems for physico-chemical properties and in vitro release as well as in vivo transdermal enhancement potential of the penetration enhancers such as cineole and oleic acid for improvement of bioavailability of drug and reducing toxic effects.

EXPERIMENTAL METHODS

Materials

Stavudine was gift sample from Matrix Laboratories Limited, Hyderabad, India. Chitosan was purchased from Marine Chemicals, Cochin, India. SodiumTPP and oleic acid were purchased from Loba Chemie Pvt. Ltd. Mumbai, India. Cineole was purchased from Sigma-Aldrich, USA. Glacial acetic acid was purchased from Merck Chemicals, India. All other reagents were analytical grade and used as such.

Animals

The animal skin was prepared using a protocol reported earlier (18). Male Wistar rats (250±10 g) were sacrificed by ether inhalation. The dorsal skin of animal was shaved and subcutaneous tissue was removed surgically and dermis side was wiped with isopropyl alcohol to remove adhered tissue. The skin was washed properly with phosphate buffer and used immediately.

Methodology

Preparation of chitosan blank film

Initially 2% w/w of chitosan solution was prepared in 1% (v/v) acetic acid solution, glycerin was used as a plastisizer at 20% w/w of polymer. This solution of chitosan containing plastisizer was further cross-linked with 0ml, 5ml, 10ml and 20ml of 0.1% w/v sodium TPP given in Table 1.This solution was then stirred gently for 2 hrs. The films were cast onto glass moulds by freeze-drying method. Chitosan film was prepared using 2% w/w chitosan in 1% v/v acetic acid solution. To this solution sodium TPP and Glycerin was added to improve the physical properties of the film and prepared films were characterized for moisture content, tensile strength and thickness uniformity.

Preparation of drug loaded chitosan film

2% chitosan solution was prepared in 1% acetic acid solution, glycerin was used as a plastisizer at 20% w/w of polymer. Stavudine (5%w/w of polymer) containing 5% w/w of penetration enhancers was mixed in the above polymeric solution. It was then cross-linked with 0ml, 5ml, 10ml and 20ml of 0.1% w/v sodium TPP. This solution was then stirred gently for 2 hrs. The films were cast onto glass moulds of 25 cm^2 by freeze-drying method. At the end of the drying period a clean blade was inserted and run along the edges of film. The film was then lifted off the mould. The dried films were wrapped in butter paper and aluminum foil and stored under vacuum. (21)

Table 1 Preparation of blank Chitosan films and drug loaded Chitosan films

Formulation	Stavudine (%w/w of polymer)	Polymer (%w/w) in 1% v/v Acetic acid solution	Sod. TPP (in ml)	Plasticiser (20% w/w of polymer)	Permeation enhancer (5% v/v)
F1		2%	0	Glycerin	
F2		2%	5	Glycerin	
F3		2%	10	Glycerin	

F4		2%	20	Glycerin	
F5	5%	2%	0	Glycerin	
F6	5%	2%	5	Glycerin	
F7	5%	2%	10	Glycerin	
F8	5%	2%	20	Glycerin	
F9	5%	2%	5	Glycerin	Cineole
F10	5%	2%	5	Glycerin	Oleic acid

Evaluation of Blank films and drug loaded films

Physical appearance

The prepared patches were physically examined for colour, clarity and surface texture.

Flim thickness

The thickness of patches was measured by using electronic caliper, with a least count of 0.01 mm. Thickness was measured at three differ ent points on the film and average readings were taken. Results obtained are shown in Table 2.

Mechanical property measurement

The mechanical properties of chitosan films were evaluated using an Ultra Test (Mecmesin, Japan). Film strip in dimension of 10 mm by 50 mm and free from air bubbles or physical imperfections was held between two clamps positioned at a distance 30 mm. During measurement top clam at a rate of 0.5 mm/s pulled the film to a distance of 50 mm before returning to the starting point. The force was measured when the films breaks. Measurements were run four times for each film. The tensile strength was calculated as:

$$\text{Tensile Strength (N/mm}^2\text{)} = \frac{\text{Breaking Force (N)}}{\text{Cross-section area of the sample (mm}^2\text{)}}$$

Results obtained are shown in Table 3.

Percentage Moisture content

The moisture content was determined by keeping membranes in a desiccator contained fused calcium chloride. The percentage moisture uptake was calculated as the difference between initial and final weight with respect to final weight.

Percentage of moisture content = [Initial weight – Final weight/Final weight] x100

Results obtained are shown in Table 4.

Percentage Moisture uptake

The percentage moisture uptake was calculated as the difference between final and initial weight with respect to initial weight.

Percentage of moisture uptake = [Final weight – Initial weight/Initial weight] x100

Results obtained are shown in Table 4.

Water vapour transmission

For this study vials of equal diameter were used as transmission cells. These cells were washed thoroughly and dried in an oven. About 1 gm of fused calcium chloride was taken in cells and the polymeric patches measuring 1 cm^2 area were fixed over the brim with the help of an adhesive. The cells were weighed accurately and initial weight was recorded, and then kept in a closed desiccator containing saturated solution of potassium chloride to maintain 80-90% RH. The cells were taken out and weighed after 24 hrs. The amount and rate of water vapour transmitted was calculated by the difference in weight using the formula. Water vapour transmission rate is usually expressed as the number of grams of moisture gained/(hr.cm^2)

WVTR = Final weight – initial weight/Time x area x 100

Results obtained are shown in Table 5.

Swelling Index

Weighed pieces 1x1 cm^2 of film were immersed in medium. Soaked films were removed from the medium at predetermined time, blotted to remove excess liquid and weighed immediately. The swelling index was calculated from the weight increase, as follows.

Swelling Index = (W2-W1)/ W1

Where, W1 and W2 are the weight of the film before and after immersion in the medium, respectively. Results obtained are shown in Table 6.

Folding endurance

The folding endurance was measured manually for the prepared patches. A strip of patch (2 x 2 cm^2) was cut and repeatedly folded at the same place till it broke. The number of times the film could be folded at the same place without breaking gave the value of folding endurance given in Table 7.

Drug content

The drug loaded chitosan films 1cm^2 area were cut from various regions and dissolved in 5

ml of the casting solvent and the volume was adjusted to 50 ml with phosphate buffer pH 7.4. It was sonicate for 3 hrs and filtered through 0.45µ membrane filter. The solution was then, suitably diluted, and content per film was estimated spectrophotometrically at 266.5 nm using standard curve. Results obtained are shown in Table 8.

Weight Variation Test

Disc of 1 cm^2 were cut from the film and weights of each determined using Mettler Toledo digital balance (Switzerland) with sensitivity upto 1mg. Results obtained are shown in Table 9.

Content Uniformity Test

To ensure uniform distribution of drug in film, a content uniformity test was performed. 10 disc of 1cm^2 area were cut from drug-loaded film and each dipped in sufficient quantity of casting solvent and the volume was adjusted to 50 ml with Phosphate buffer pH 7.4. It was sonicate for 3 hrs and filtered through 0.45µ membrane filter. The solution was then, suitably diluted, and content per film was estimated spectrophotometrically at 266.5 nm using standard curve. Results obtained are shown in Table 9.

Differential Scanning Colorimetry (DSC)

Thermograms of pure Stavudine, chitosan and chitosan film were obtained using Mettler - Toledo DSC 821^e (Mettler –Toledo, Switzerland) equipped with intracooler. Indium/Zinc standards were used to calibrate DSC temperature and enthalpy scale. Weighed sample of Stavudine, chitosan and chitosan film were hermetically sealed in aluminum pans and heated at a constant rate of 10 ^oC/min, over a temperature of 25-250 ^oC. Inert atmosphere was maintained by purging nitrogen gas (flow rate, 50 ml/min) (21).

Fourier Transform Infrared Spectroscopy (FTIR) measurements

FTIR spectra of Stavudine loaded film were recorded on (Jasco V-5300, Japan) in the range of 500 to 3500 cm^{-1} in KBr pellets prepared on KBr press (Spectra lab, India). For comparison, FTIR spectrum of pure Stavudine and chitosan was also recorded.

Scanning Electron Microscopy (SEM)

Samples for SEM studies were mounted on the specimen slubs using fevicol adhesive. Small samples were mounted directly using scotch double adhesive tape. Samples were coated with gold to the thickness of 100 A0 using Hitachi vacuum evaporator (model HUS5GB). Coated

samples were analyzed in Hitachi Scanning Electron Microscope model S-450 operated at 1.2kv and photographed.

X-ray Diffraction (XRD)

Molecular arrangement of Stavudine and chitosan in powder as well as in films was compared by powder x-ray diffraction patterns acquired at room temperature on a Philips PW 3710 diffractometer (Eindhoven, Netherland). The data were collected over an angular range from 3^0 to 50^0 2θ in continuous mode using a step size of 0.02^0 2θ and step time of 5 seconds.

***In- vitro* diffusion and Ex- *vivo* permeation study using rat skin**

To see the pattern of Stavudine release from the different formulations, diffusion studies were carried out using cellulose membrane and rat skin. All formulations were subjected to *in vitro* diffusion through cellulose membrane by using Franz diffusion cell with diffusional surface area of 3.14 cm^2 and a receptor volume of 18 ml. Cellulose membrane was used as barrier between donor and receptor compartment. The membrane was mounted on a Franz diffusion cell. The receptor compartment was filled with phosphate buffer pH 7.4. It was jacketed to maintain the temperature 37 ± 0.5 ^{0}C and was kept under constant stirring. Prior to application, the membrane was allowed to equilibrate at this condition for 30 min. Ex-vivo permeation studies across rat skin were carried out using a permeation set up described above except that instead of cellulose membrane, rat skin was used. The skin pieces were mounted over diffusion cells with the dermal side in contact with the receptor phase, equilibrated for 2 h. Magnetic stirrer at 300 rpm stirred the receptor fluid in each cell. 1 cm^2 area of drug-loaded film was clamped between donor and receptor compartments against rat skin. Samples were withdrawn at definite time intervals from the receptor compartment followed by replacement with fresh volume of phosphate buffer solution and concentration of Stavudine in receptor samples was analyzed by UV spectrophotometric method. For each skin specimen, Stavudine permeated per unit area was calculated and plotted against time.

Permeation Data Analysis

- Drug release kinetics
- Flux
- Enhancement ratio (ER)

Drug release kinetics

The results of *in vitro* permeation studies are subjected for different kinetic models such as zero order, first order, Higuchi and Korsemeyer and Peppas equations. The regression coefficient values were given in Table 10.

Flux

The flux (µg $cm^{-2}hr^{-1}$) was calculated from the slope of the plot of the cumulative amount of drug permeated per cm^2 of skin at steady state against the time using linear regression analysis. In steady state situation, the flux J, is defined as the slope of line.

$$J = dQ/dtA$$

Enhancement ratio (ER)

Enhancement ratio was used to evaluate the effect of permeation enhancer on diffusion and permeation of selected drug molecules. It is calculated by:

Enhancement Ratio = Kp with permeation enhacer/ Kp without permeation enhancer

Results of flux and enhancement ratio were given in Table 12.

Skin irritation studies

A primary skin irritation test was performed on six healthy rats, weighing between 150-200gms. The patch of area 3.14 cm^2 was used as a test patch. The dorsal surface of rabbits was cleared well and the hair was removed by using a depilatory preparation. The skin was cleared with rectified spirit. The transdermal patch was placed on the dorsal surface of the abdominal skin with the help of an adhesive tape. The patches were removed after 24 hr and the skin was examined for erythema and edema.

Stability

The stability studies were conducted according to International Conference on Harmonization guidelines by storing the transdermal films at 40±2°C with 75% RH in stability chamber for 3 months. The samples were withdrawn after 3 months and analyzed for drug content in UV spectrophotometer.

RESULTS AND DISCUSSION

The patches formed were smooth and translucent in appearance.

Thickness uniformity test

It was observed that increasing the concentration of cross-linking agent then there were increase in the thickness of the film as shown in Table 2. Thickness of the films was

increased due to the cross-linking of the Sodium TPP with chitosan polymer. The batches from F5 to F10 were containing drug shows decrease in the thickness because of the interaction of the drug with chitosan polymer. Formation of a compact structure during freeze drying and less porous as observed from SEM studies later.

Table 2 Film thickness of blank cross-linked films and drug loaded films

Formulation Code	Trial 1 mm	Trial 2 mm	Trial 3 mm	Mean ± S.D.
F1	0.87	0.90	0.90	0.89 ± 0.01
F2	0.92	0.90	0.94	0.92 ± 0.02
F3	0.94	0.96	0.96	0.95 ± 0.01
F4	0.96	0.97	0.99	0.97 ± 0.02
F5	0.86	0.89	0.89	0.88 ± 0.01
F6	0.91	0.89	0.93	0.91 ± 0.02
F7	0.93	0.95	0.95	0.94 ± 0.01
F8	0.95	0.96	0.98	0.96 ± 0.02
F9	0.90	0.88	0.92	0.90 ± 0.02
F10	0.87	0.85	0.89	0.87 ± 0.02

Mechanical property of the film

The tensile strength testing provides an indication of the strength at the film. It is suggested that films suitable for transdermal drug delivery should preferably be strong but flexible. The mechanical properties are given in the Table 3. Increasing the concentration of cross-linking agent from 0 ml to 20 ml increased the tensile strength of the film. The tensile strength of film was increased due to the formation of complex with the chitosan polymer. More the concentration of the cross-linking agent more will be the formation of ionic cross-linking and hence the tensile strength is also high.

Table 3 Tensile strength of blank Cross-linked films and cross-linked films containing Plastisizer with Drug

Film code	Tensile strength (N/mm^2)	± SD
F1	0.0180	0.003808
F2	0.0271	0.004848
F3	0.351	0.003162
F4	0.0499	0.004899
F5	0.0134	0.000574
F6	0.0265	0.00222
F7	0.0320	0.002051
F8	0.0496	0.007127
F9	0.0261	0.000304
F10	0.0259	0.002051

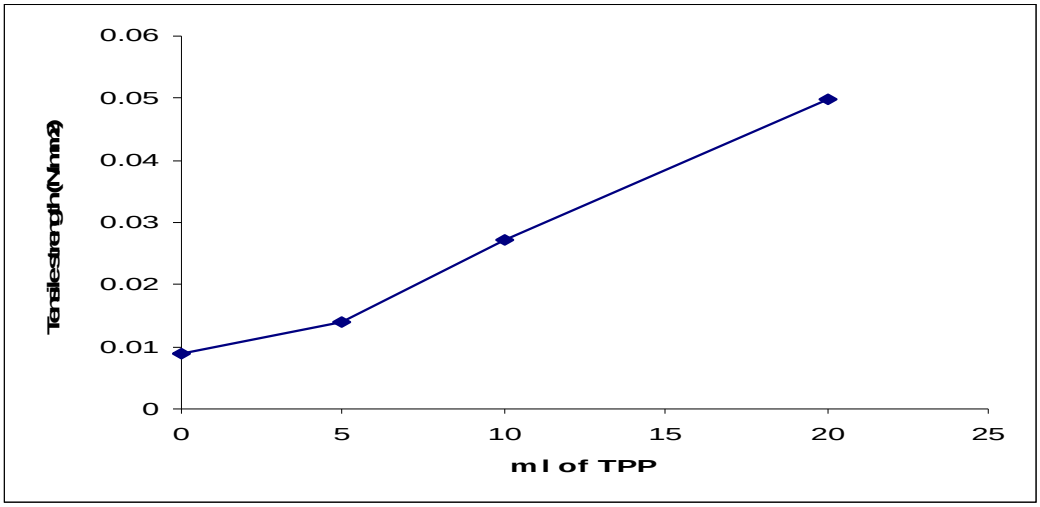

Figure 1 Effect of TPP on tensile strength of blank chitosan film

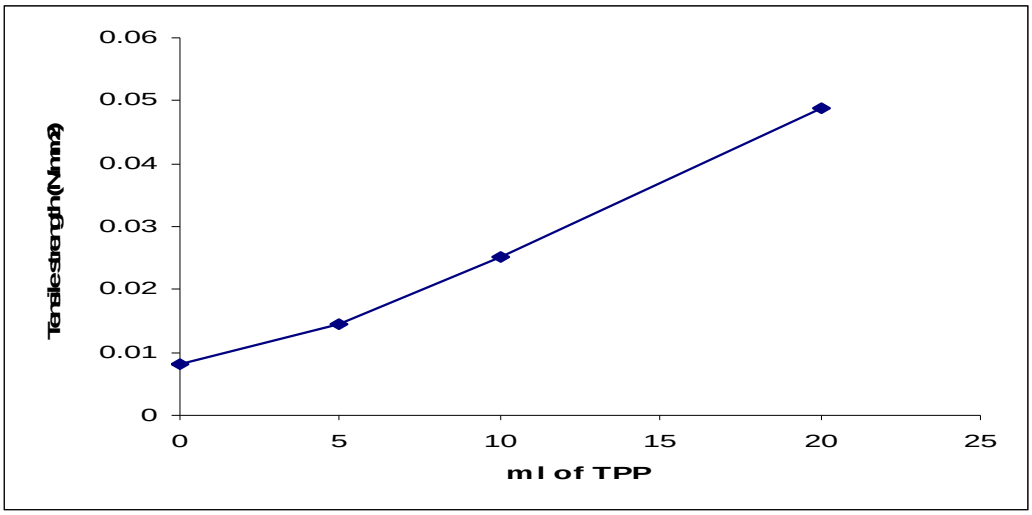

Figure 2 Effect of TPP on tensile strength of Cross-linked films with Plastisizer and Drug

The tensile strength of the films containing glycerin as a plastisizer was flexible because glycerin may have decreased the rigidity of the network, providing a less ordered film structure and increasing the ability of movement of polymer. Thus glycerin acts as a better plastisizer used in the same concentration.

% Moisture content and moisture uptake

The moisture present in the matrix films helps in maintaining suppleness thus preventing drying and brittleness. Low moisture uptake protects the films from the microbial contamination as well as bulkiness of the transdermal patch. CH contains free –NH2 groups. Interactions of different functional groups with these moieties are utilized in modifying drug release. Also, this –NH2 group gains positive charge when dissolved in acidic medium. On the other hand, NaTPP dissolved in water dissociate to give phosphoric ions. The cross-

linking of CH is known to be dependent on the availability of the cationic sites and the negatively charged species. Therefore, two concentrations of CH and various concentrations of NaTPP was used to study the relationship between moisture content, moisture uptake and cross-linker concentration. Moisture content, moisture uptake of CH films, mainly influenced by ionic interactions between CH chains, is reported to depend formation of the network. An increase in cross-linking density is reported to induce a decrease in moisture content and moisture uptake. These results support that the more tightly cross-linked chitosan matrix does not swell (lower water uptake) as much as the loosely cross-linked chitosan matrix. At lower volume of TPP (e.g., lower cross-link density), the chitosan network is loose and has a high hydrodynamic free volume to accommodate more of the solvent molecules, thereby inducing chitosan–TPP matrix swelling. The water uptake in hydrogels depends upon the extent of hydrodynamic free volume and availability of hydrophilic functional groups for the water to establish hydrogen bonds. Higher water uptake values at lower levels of cross-linking and vice versa observed in the present study confirm the formation of rigid chitosan-TPP networks through the present preparation process.

Table 4 Moisture contentand moisture uptake in blank cross-linked films and drug loaded films

Film code	Moisture content (%) ± SD	Moisture uptake (%) ± SD
F1	46.68 ± 0.68	27.70 ± 0.62
F2	45.61 ± 0.26	24.70 ± 0.54
F3	44.57 ± 0.61	18.83 ± 0.49
F4	35.10 ± 0.58	15.62 ±0.52
F5	43.88 ± 0.67	25.23 ± 0.44
F6	41.69 ± 0.76	23.78 ± 0.65
F7	40.77 ± 0.41	16.52 ± 0.44
F8	34.14 ± 0.43	14.77 ±0.55
F9	42.39 ± 0.74	22.55 ± 0.33
F10	40.62 ± 0.89	23.22 ± 0.11

Water vapour transmission rate

Both uncrosslinked polymeric films were water soluble whereas the crosslinked films were water insoluble but permeable to water vapor. Chitosan films showed water vapor transmission rates ranging from 2.31 ± 0.06 mg/hr.cm^2 (uncrosslinked film) to 0.96 ± 0.03 (crosslinked film with 5%, 10% and 20% w/v TPP) are given in Table 5. The permeability of chitosan films to water vapor could be controlled by the crosslinking concentration.

Table 5 Water vapour transmission rate in drug loaded film

Film Code	WVTR ± SD [mg/(hr.cm^2)]
F1	2.31 ± 0.06
F2	1.97 ± 0.01
F3	1.21 ± 0.02
F4	0.96 ± 0.03
F5	1.96 ± 0.20
F6	1.95 ± 0.21
F7	1.97 ± 0.33
F8	1.95 ± 0.18
F9	1.93 ± 0.22
F10	1.92 ± 0.33

Swelling Index

The % swelling index was determined and found to high from F5 to low F10 with different % of crosslinking agent. The result from the table6, clearly indicates that as the time increases the % swelling index increases.

Table 6 % Swelling index in drug loaded film

Film Code	% Swelling Index							
	1hr.	2hr.	3hr.	4hr.	5hr.	6hr.	7hr.	8hr.
F1	68.1	72.2	73.5	75.9	77.1	78.7	79.6	80.4
F2	65.4	68.3	71.2	74.1	75.5	76.1	77.7	78.1
F3	63.5	66.2	69.1	71.3	73.1	75.2	76.5	77.2
F4	60.5	63.2	66.1	69.3	72.1	74.2	75.5	76.2
F5	58.5	60.2	62.1	64.3	65.1	66.2	67.5	68.2
F6	59.5	61.2	62.1	63.3	64.1	65.2	66.5	67.2
F7	60.5	62.2	63.1	64.3	65.1	66.2	67.5	68.2
F8	61.5	63.2	65.1	67.3	69.1	71.2	72.5	73.2
F9	58.5	60.2	61.1	62.3	63.1	65.2	65.7	66.2
F10	57.5	59..2	60.1	61.3	62.1	64.2	64.9	65.2

Folding endurance

The recorded folding endurance of the patches was shown in Table 7. It depicits all formulations have good film properties. The folding endurance of the patches were containing enhancers decreases the folding endurance of the patches. This test is important to check brittleness, less folding endurance indicates more brittleness.

Table 7 Folding endurance data of patches

Film code	Trial 1	Trial 1	Trial 1	Mean ± SD
F1	150	165	158	157.66 ± 7.505
F2	113	129	125	122.33 ± 8.326
F3	106	109	103	106 ± 3.0
F4	104	92	97	98 ± 6.027
F5	76	76	67	72.66 ± 4.932
F6	86	89	93	89.33 ± 3.511
F7	99	91	95	95 ± 4.0
F8	82	76	88	82 ± 6
F9	85	88	92	88.33 ± 3.511
F10	84	87	91	87.33 ± 3.511

Drug content in the film

The % drug content of all formulations were more than 92.65 ± 2.84 indicating good loading efficacy and suitability of method adopted for preparing chitosan film. There was no significant difference in drug content was observed within the studied batches given in Table 8.

Table 8 Drug content in the film

Film code	Area of the film (cm^2)	Loaded drug content (mg)	% Drug content ± SD
F5	25	35	94.19 ± 1.75
F6	25	35	95.99 ± 0.75
F7	25	35	93.94 ± 0.37
F8	25	35	92.65 ± 2.84
F9	25	35	95.88 ± 0.95
F10	25	35	95.93 ± 0.71

Content and weight uniformity test

In the formation of film there was very less drug loss during the process, which is shows in Table 9. It shows that the films have uniformity in its weight and drug content.

Table 9 Weight variation and content uniformity test for drug loaded film

Film code	Weight (mg)	± SD	Drug content (mg)	± SD
F5	1.51	0.11	1.318	0.01
F6	1.52	0.13	1.343	0.01
F7	1.49	0.08	1.315	0.01
F8	1.53	0.21	1.297	0.02
F9	1.50	0.31	1.342	0.01
F10	1.55	0.24	1.343	0.02

Thermal Studies of Films

The DSC thermograms of stavudine, chitosan flakes, chitosan films and stavudine -chitosan films are shown in Figure 3. DSC studies were performed to understand the behaviour of the stavudine, cross-linked chitosan & drug loaded chitosan on application of thermal energy. Chitosan flakes showed broad endotherm from 57.16^{0}C to 114.68^{0}C indicating moisture loss from the sample. The endotherm related to evaporation of water is expected to reflect the molecular changes brought in after cross-linking. DSC thermogram of blank chitosan film showed broad endotherm from 78.43^{0}C to 136.59^{0}C indicating moisture loss from the sample. DSC thermogram of stavudine showed a sharp endotherm peak that corresponds to melting in the range of 171.17^{0}C (22). However this endothermic peak shifted to 170.11^{0}C in case of stavudine -chitosan films. The DSC analysis of the drug loaded and drug free films (Figure 3) revealed a negligible change in the melting point of stavudine in the presence of the polymers, indicating the stable nature of stavudine in the presence of polymers.

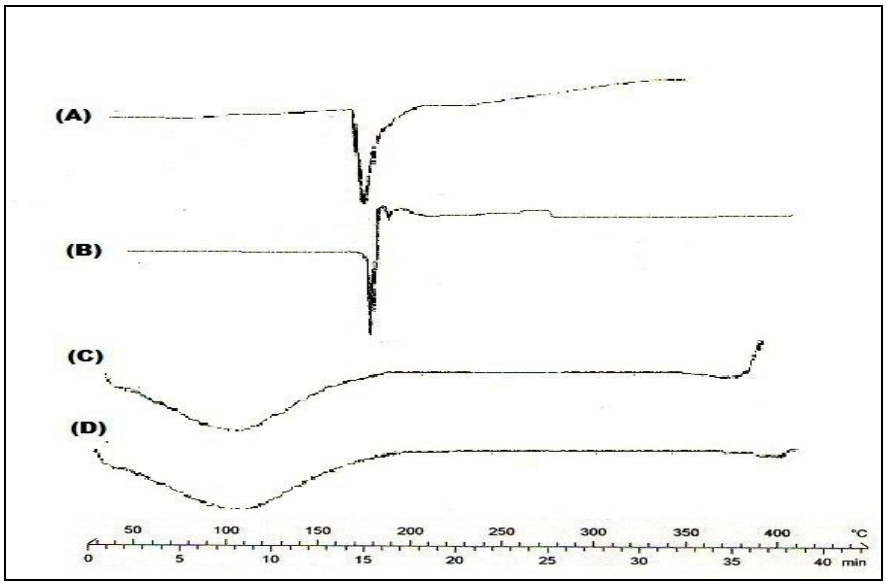

Figure 3 DSC of A) Stavudine, B) Stavudine –chitosan film. C) chitosan flakes, and D) Blank chitosan film

Fourier Transform Infrared Spectroscopy Measurements

Transmission infrared spectra of chitosan powder, stavudine and stavudine film were acquired to draw information on the molecular state of chitosan and stavudine. Chitosan is an amino glucose characterized by a small proportion of amide groups via as a amide linkage with acetic acid. In the infrared spectrum, powder chitosan exhibited a broad peak at 3431 cm^{-1}, which is assigned to the N-H and Hydrogen boned O-H stretch vibrational frequencies

while a sharp peak at 3610 cm^{-1} is that of free O-H bond of glucopyranose units .Further, in the C-H stretch region of FTIR spectrum, the higher intensity peak at 2923 cm^{-1} is assigned to the asymmetric and the lower intensity peak at 2857 cm^{-1} is assigned to the symmetric modes of CH_3. The peaks at 1550 and 1599 cm^{-1} were assigned to strong N-H bending vibrationsof secondary amide, which usually occur in the range of 1640 to 1550 cm^{-1} as strong band (23). The spectra of pure stavudine, pure Chitosan, stavudine loaded chitosan film are shown in figure 4. The FTIR characteristic stavudine bands are -OH stretching at 3426 cm^{-1}, -NH stretching at 3169 cm^{-1}, Ar-CH=C stretching at 3043 cm^{-1}, CH_2 and CH_3 stretching at 2882 cm^{-1} and 2821 cm^{-1}, C=O stretching at1691 cm^{-1} and -NH bending at 1264 cm^{-1} (24). Spectra of pure chitosan showed a strong band at 1710 cm^{-1} which is characteristic peak of non-ionized carboxylic group and the spectra of stavudine loaded chitosan film showed the characteristic peak of carbonyl group at 1691 cm^{-1} and azide group at 1264 cm^{-1} indicated that the stable nature of stavudine in film formulation with no chemical interaction between chitosan and stavudine.

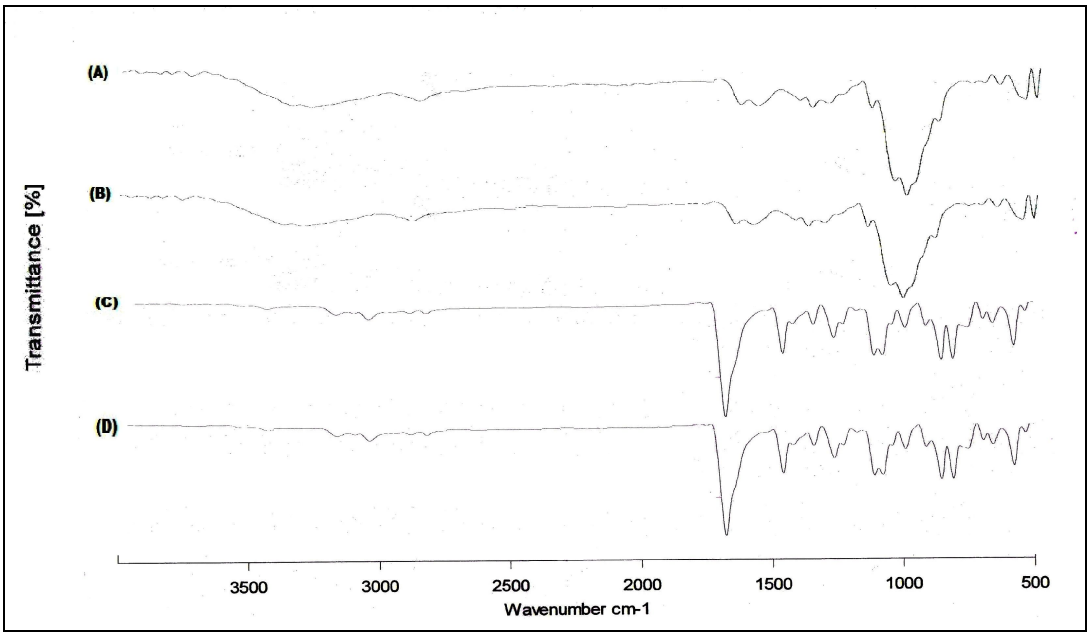

Figure 4 FTIR spectra of (a) Chitosan, (b) Blank chitosan film, (c) Drug (d) Drug loaded chitosan film

Film morphology studies

SEM microphotographs revealed that sample of stavudine has a rough surface, as shown in Figure 5 A.

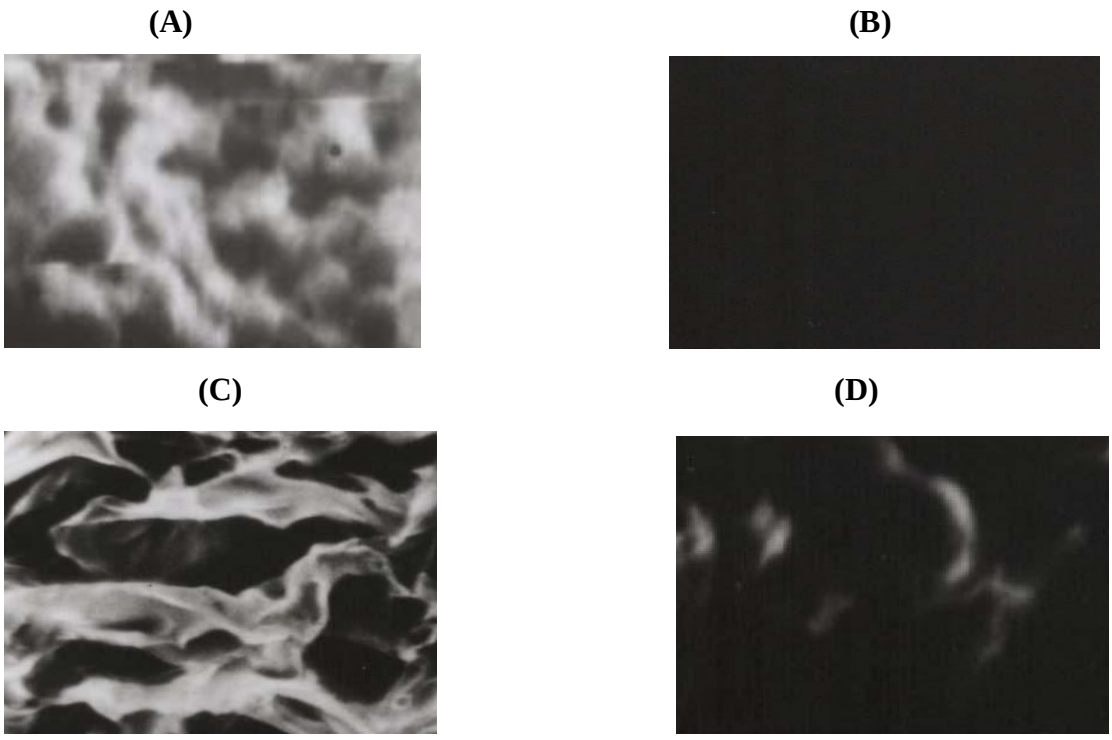

Figure 5 Scanning Electron Photomicrographs of A) Stavudine, B) Blank film, C) Stavudine – Chitosan film, D) Stavudine – Chitosan film after diffusion. Magnification: A) x 180, B) x 900, C) x 180, D) x 180

In addition, SEM microphotographs of blank film and stavudine films were acquired and compared with that of stavudine sample.The morphology of blank film was plain, indicating that the blank film had a smooth surface (Figure5 B). In contrast to the blank film, features of stavudine-chitosan film showed rough surface as compared to blank film (Figure 5 C). This typical surface appearance suggests that stavudine is not only dispersed in the film matrix but also projected onto the surface of the film. After diffusion of stavudine the morphology of stavudine-chitosan film showed smooth surface (Figure 5 D).

X-Ray Diffraction

The X-ray powder diffraction pattern of pure drug has shown its own characteristic crystal peaks between 2θ of 10^0 and 80^0. Whereas characteristic peaks of drug were absent in chitosan film indicating probable decreased crystallinity of the drug. The undefined broad, diffused peaks withthelow intensities for drug loaded film indicate the conversion of crystalline to amorphous state of drug in formulation (25).

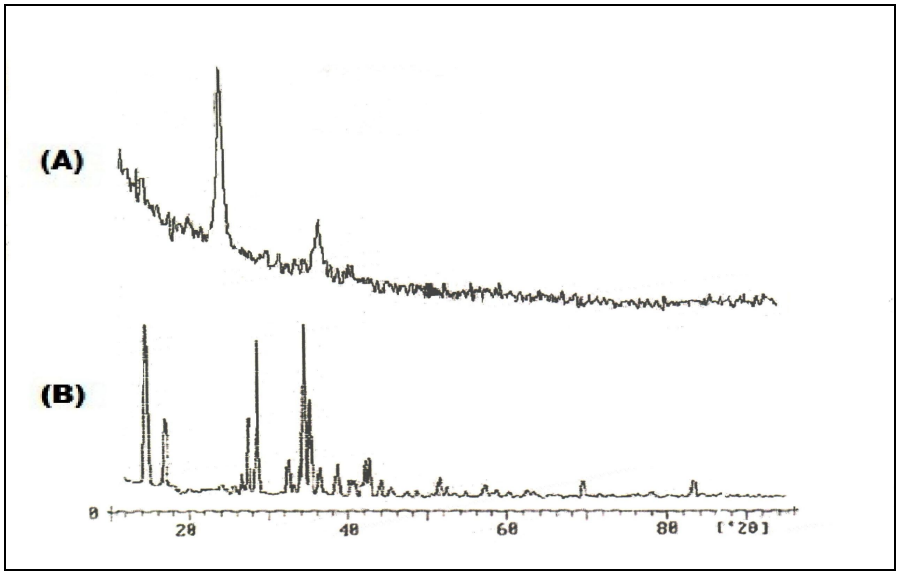

Figure 6 XRD of (A) Stavudine loaded crosslinked film, (B) Stavudin

***In-vitro* and *Ex- vivo* Permeation study**

The in-vitro diffusion studies were carried out as described earlier. The amount of drug diffused from F5, F6, F7, F8, F9 and F10 are shown in Figure7. The drug diffused from F6 was more as compared to F5, F7 and F8 because of low concentration (5 ml of TPP) of cross-linking agent. Increase in the concentration of cross-linking agent leads to as increase in the density of the cross-linked network of chitosan. Due to the more complex network formed in the F7 and F8, the drug diffused from these films were low. On the basis of drug diffusion F6 was selected for incorporating enhancers to increasse drug diffusion for further study. All the enhancers formulated at 5% (w/w) in chitosan film increase the penetration of Stavudine through the skin. All the molecules tested increase Stavudine flux relative to control F6. All enhancers studied do not increase Stavudine flux to the same extent. Oleic acid significantly increases the flux of Stavudine across the skin respective to the control. Oleic acid has been found to increase the epidermal permeability through a mechanism involving the stratum corneum lipid membranes. Oleic acid is incorporated into skin lipid, disrupts molecular packaging and alters the level of hydration, thus allowing drug penetration (26). It has also been described that at high concentrations oleic acid can exist as a separate phase within the lipid bilayers (27, 28). Our results confirm that it can work synergistically with glycerol, as proposed by other authors (29). It has shown a moderate enhancing activity on the transdermal flux of Stavudine, probably due to its moderate capacity for disrupting the stratum corneum lipid packing. It was reported that oxygen containing terpenes, such as cineole etc form new aqueous pore pathways in the skin thus increasing the permeation of

hydrophilic drugs like Stavudine (30). According to the lipid protein and partitioning theory, penetration enhancers may act by one or more of the three main mechanisms: disruption of the highly ordered lipid structure, interaction with intracellular protein to promote permeation through the corneocyte and increased partitioning (31). As terpenes are highly lipophillic, it is less likely that they interact with keratin, which has been proved by calorimetric studies where they did not alter protein endotherm (31-32). On the other hand, it was found that terpenes alter neither thermodynamic activity nor partioning of Stavudine into stratum corneum from vehicle (33). Hence, the only other possible mechanism was disruption/alteration in the barrier property of stratum corneum. So oxygen containing terpenes, such as cineole predominantly act as, first by disrupting the existing lateral/transverse hydrogen bond network of the stratum corneum lipids bilayer probably by preferential hydrogen bonding of terpenes with ceramide head groups and secondly by facilitating the excessive hydration of ceramide head groups and thereby increase the breath of existing polar pathways or form new polar pathways.

Maximum drug diffusion was observed from F10 containing 5% oleic acid and F9 containing 5% cineole were added as penetration enhancers while minimum drug diffusion was observed from F6 (Control) are illustrated Figure 8. It was observed that only 263µg/cm^2 of drug diffused from control preparation F6 in 10 h which is not sufficient to achieve and maintain therapeutic concentration of stavudine. So diffusion of stavudine can be significantly enhanced by penetration enhancer 5% oleic acid and 5% cineole. At 5% w/w enhancer concentration, diffusion of stavudine increased from 263 µg/cm^2 to 969 µg/cm^2 in F10 containing 5% oleic acid and 778 µg/cm^2 in F9 containing 5% cineole attained in 10 h which is sufficient to achieve and maintain therapeutic concentration of stavudine from chitosan film formulations.

Flux values of stavudine from different formulations in decreasing order are as follows F10> F9 > F6 (Control). Flux of stavudine is different from control and other formulations. However among these enhancers, flux of stavudine with of 5% oleic acid and 5% cineole were maximum and not significantly different from each other in their flux enhancement activities, although 5% oleic acid showed higher flux values. These flux values were above the theoretical stavudine flux values (0.2 and 0.6 mg/cm^2/h) (34). The steady state flux of stavudine from film formulation calculated from the linear portions of the cumulative amount permeated against time plots was 33µg/cm^2/h from F10 respectively and the flux values were

very high in comparison with passive stavudine flux across rat skin in the absence of ethanol and penetration enhancers (35).

According to the lipid protein and partitioning theory, penetration enhancers may act by one or more of the three main mechanism : disruption of the highly ordered lipid structure, interaction with intracellular protein to promote permeation through the corneocyte and increased partitioning (36). As terpenes are highly lipophilic it is less likely that they interact with keratin, and it has been proved by calorimetric studies where they did not alter protein endotherm (37). On the other hand, it was found that terpenes alter neither thermodynamic activity nor partioning of stavudine in to SC from vehicle (38). Hence, the only other mechanism possible is disruption/alteration in the barrier property of SC. So oxygen containing terpenes, such as menthol, cineole predominantly acting as: 1) disrupt the existing lateral/transverse hydrogen bond network of the SC lipids bilayer probably by preferential hydrogen bonding of terpenes with ceramide head groups 2) Facilitate the excessive hydration of ceramide head groups and thereby increase the breath of existing polar pathways or form new polar pathways.

As the steady state flux of Stavudine across rat skin from formulation F10 was above 33µg/cm^2/h, from 1cm^{2}area achieving therapeutically effective plasma concentrations would be possible with these formulations.

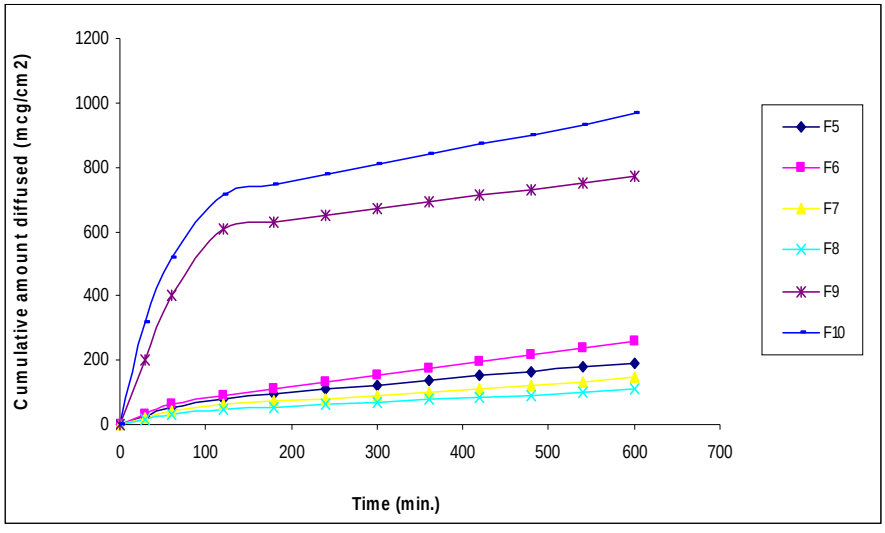

Figure 7 Drug diffused from different formulations through cellophane membrane

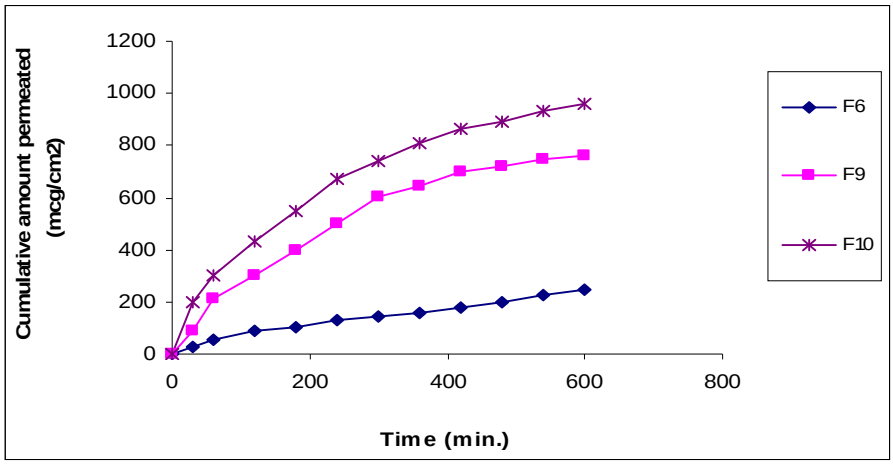

Figure 8 Ex vivo permeation profiles of Stavudine across rat skin from films

Drug release kinetics graphs

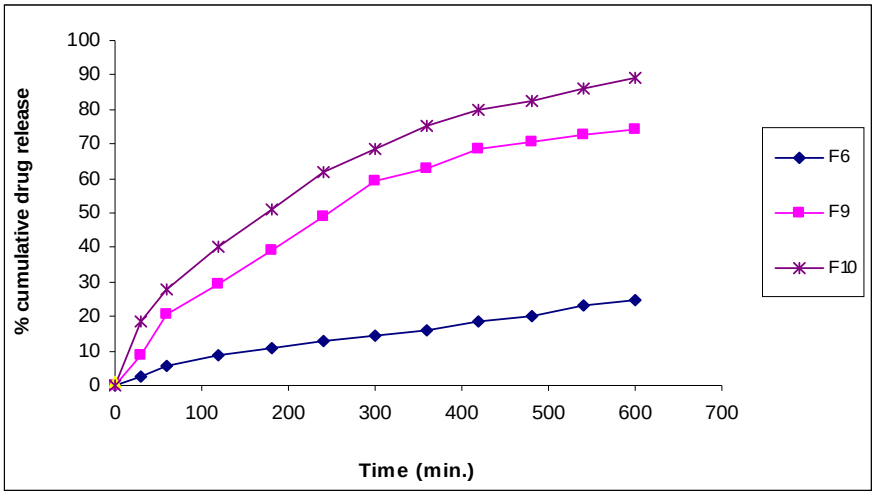

Figure 9 Zero order release kinetic profile of Stavudine loaded patches

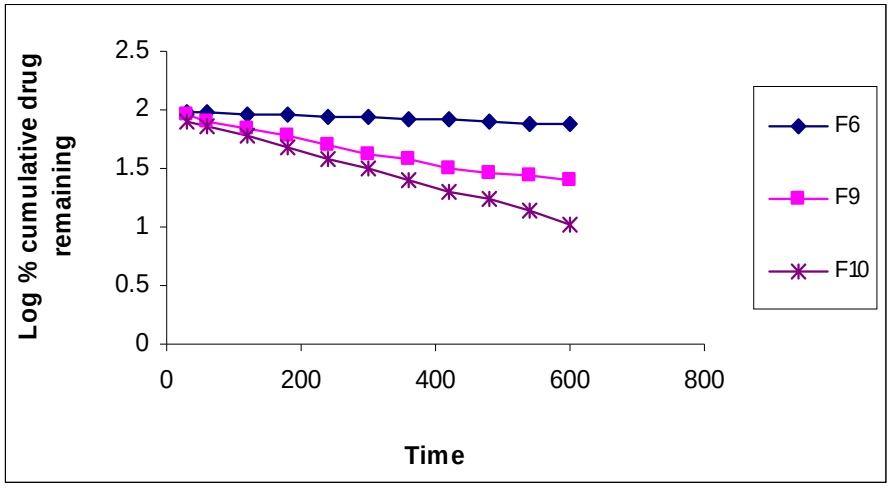

Figure 10 First order release kinetic profile of Stavudine loaded patches

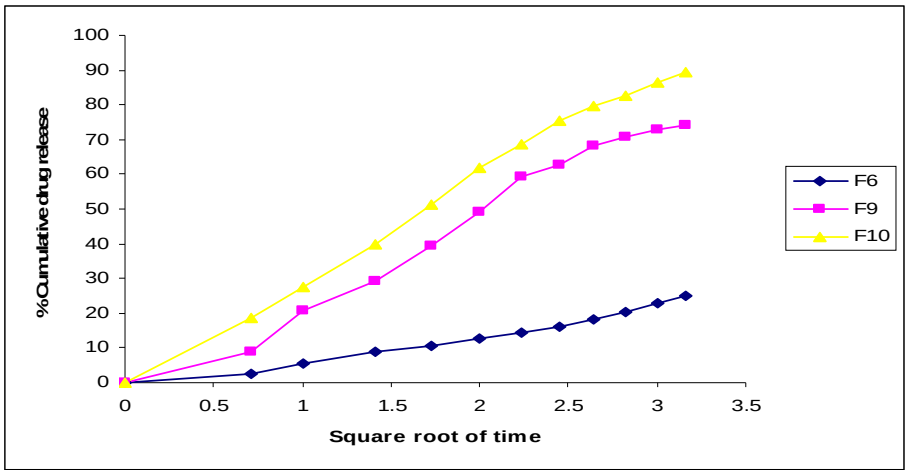

Figure 11 Higuchi release kinetic profile of Stavudine loaded patches

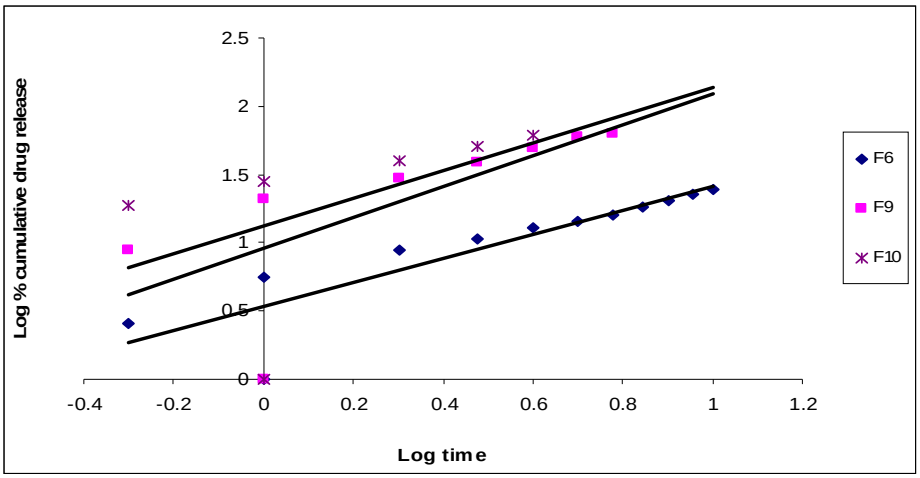

Figure 12 Peppas release kinetic profile of Stavudine loaded patches

Table 10 Drug release kinetics of Stavudine from the films

Formulation code	Zero order	First order	Higuchi matrix	Peppas kinetics	'n' values for peppas
F6	0.977	0.990	0.978	0.806	0.878
F9	0.918	0.977	0.983	0.623	1.131
F10	0.907	0.999	0.977	0.502	1.016

The release kinetics was evaluated by making use of zero order, first order Higuchi's diffusion and Korsemeyer -Peppas equation. Calculated regression coefficient values for different formulations are tabulated in Table 10. These values are compared with each other for model and drug equation. Based on the higher regression values (r^2) the best fit model was first order for formulations F6 and F10 formulations, whereas higuchi's matrix release for F9 formulation. The Figure 9 - 11 **s**hows release kinetic profile of stavudine patches for zero order, first order, Higuchi and Peppas respectively.

The Peppas model is widely used when the release mechanism is not well known or when more than one type of release phenomenon could be involved. 'n' value could be used to characterize different release mechanism. Peppas-Korsmeyer equation is given as,

% R= K tn

Or

Log %R= Log k + Log t

Where, R= drug release, K= constant, n= slope, t= time

Table 11 Mechanism of drug release

'n'	Mechanism
n<0.5	Fickian diffusion
0.5 < n < 1	Non fickian diffusion
Above 1	Case II transport

The 'n' values obtained graphically from peppas plot were shown in Table 11. The values obtained between 0.878 to 1.131 which indicates that the release approximates non fickian diffusion and case II transport.

Flux and Enhancement ratio

Table 12 Permeation parameters of Stavudine through rat skin

Formulations	Steady stateFlux (µg /cm^2/h)	Enhancement ratio
F6	38.2	1
F9	122.4	3.13
F10	136.2	3.31

Skin Irritancy Study

Results of skin irritancy study revealed that neither blank patch nor patch containing Stavudine caused any noticeable sign of erythema or edema on rat skin throughout the period of 48 h. Hence the patches were found to be compatible with the skin.]

Table 13 Skin irritancy study data

SKIN RESPONSES	SCORE
Erythema and Eschar Formation	
No Erythema	0
Very slight erythema (barely perceptible)	0
Well-defined erythema	0
Moderate to severe erythema	0
Severe erythema (beet-redness) to slight eschar formation (injuries in depth)	0

Edema formation	
No edema	0
Very slight edema (barely perceptible)	0
Slight edema (edges of area well-defined by definite raising)	0
Moderate edema (raised approximately 1.0 mm)	0
Severe edema (raised more than 1.0 mm and extending beyond exposure area)	0
Total possible score for irritation	0

Stability studies

Table 14 shows drug content of the formulations before and after stability study. These formulations were stored at 40±2°C/75%RH in stability chamber for 3 months. Drug content of the patches after stability studies did not show any significant variations. These result indicates that drug remain stable after stability studies.

Table 14 Stability Study Data of Transdermal Films

Formulation code	% Drug content ± SD before storage	% Drug content ± SD After 3 months
F9	95.88 ± 0.95	95.11± 0.21
F10	95.93 ± 0.71	95.13± 0.42

CONCLUSION

In conclusion, oleic acid was shown to be exclusively the best enhancer stavudine chitosan film as F10 when tried in 5% concentration. Also, cineole was shown to be the good enhancer for drug permeation when tried in 5% concentration compared with the control Stavudine patches. Ex-vivo drug permeation through rat skin studies, F10 (oleic acid), F9 (cineole) showed a high flux and short lag time as compared to F6 (control), so achieving therapeutically effective plasma concentrations would be possible with these formulations.

ACKNOWLEDGEMENT

Authors are thankful to matrix laboratories limited, hyderabad, india for providing gift sample of Stavudine.

REFERENCES

1. http://www.ucmp.berkeley.edu/alllife/virus.html.
2. http://www.infoplease.com/ce6/sci/A0851010.html.
3. http://emedicine.medscape.com/article/1533218-overview.
4. Alimonti JB, Blake T and Fowke KE .Mechanisms of CD4+ T lymphocyte cell death in human immunodeficiency virus infection and AIDS DOI 10.1099/vir.0.19110-0.

5. Goodman, G. 2001. *The Pharmacological Basis of Therapeutics*, Mac Millan Publishing Company, New York, p. 1357.
6. Sweetman, S.C. 2002. *Martindale, In: The Complete Reference*, Pharmaceutical Press, London, p. 641.
7. Robinson, J.R., Lee, H.L. (1987) Controlled Drug Delivery Fundamentals and Applications, 2nd ed., Marcel Decker, New York; 524-552.
8. Jain, N.K.: Controlled and Novel drug delivery. (1997), 1st edition, CBS Publisher and distributor: 100-126.
9. Ilium L. 1998. Chitosan and its use as a pharmaceutical excipient. Pharm Res.;15:1326Y1331.
10. Felt O, P Buri, R.Gurny 1998. Chitosan: a unique polysaccharide for drug delivery. Drug Dev Ind Pharm. 24:979Y993.
11. Van der Lubben IM, JC Verhoef, G Borchard, HE Junginger 2001. Chitosan and its derivatives in mucosal drug and vaccine delivery. Eur J Pharm Sci. 14:201Y207.
12. Calvo P, C Remunan-Lopez, CL Vila-Jato, MJ Alonso 1997. Novel hydrophilic chitosan-polyethylene oxide nanoparticles as protein carriers. J Appl Polym Sci.;63:125Y132.
13. Williams AC, BW. Barry, 1991. Terpenes and lipid-protein partitioning theory of skin penetration enhancement. *Pharm Res*. 8:17- 24
14. Okabe H, Y. Obata, K. Takayama, T. Nagai, 1990. Percutaneous absorption enhancing effect and skin irritation of monocyclic monoterpenes. *Drug Des Deliv*. 6:229-238.
15. Gao S, J. Singh, 1998. *In vitro* percutaneous absorption enhancement of a lipophilic drug tamoxifen by terpenes. *J Control Release*. 51:193-199.
16. Zhao K, J. Singh 1999. *In vitro* percutaneous absorption enhancement of propranolol hydrochloride through porcine epidermis by terpenes/ ethanol. *J Control Release*. 62:359-366.
17. Calvo P, C Remunan-Lopez, CL Vila-Jato, MJ Alonso 1997. Chitosan and chitosan/ethylene oxide-propylene oxide block copolymer nanoparticles as novel carriers for proteins and vaccines. Pharm Res. 14:1431Y1436.
18. Akbuga J, Durmaz G. Preparation and evaluation of cross-linked chitosan microspheres containing furosemide. IntJ Pharm. 1994; 111:217Y222.
19. Berger J, M Reist, JM Mayer, O Felt, NA Peppas, R. Gurny 2004Structure and interactions in covalently and ionically crosslinked chitosan hydrogels for biomedical applications. Eur J Pharm Biopharm. 57:19Y34.

20. Knaul JZ, SM Hudson, KAM Creber. 1999. Improved mechanical properties of chitosan fibres. J Appl Polym Sci. 72: 1721Y1731.
21. Singh Nripendra and Upasani C. D.2013. Skin Permeation of Zidovudine from Crosslinked Chitosan Film Containing Terpene Enhancers for Transdermal Use. IOSR Journal of Pharmacy and Biological Sciences,. Volume 7, Issue 2 ,PP 31-35.
22. Berger J, M Reist, JM Mayer, O Felt, NA Peppas, R. Gurny 2004Structure and interactions in covalently and ionically crosslinked chitosan hydrogels for biomedical applications. Eur J Pharm Biopharm. 57:19Y34.
23. Dhanikula, A.B., Panchagnula, R., 2004. Development and Characterization of Biodegradable Chitosan films for Local Delivery of Paclitaxel. AAPS 6(3), 1-12.
24. Aktar, B.; Erdal, M.S.; Sairli, O.; Güngör, S.; Özsoy, Y. Transdermal films of metoclopramide hydrochloride with terpenes as penetration enhancers: Design, characterization, *in vitro* evaluation and ATR-FTIR spectroscopic investigation on excised pig skin. *Asian Chem. Lett.* **2011**, *16*, 67–78.
25. Mundargi, R.C., Babu, V. R., Rangaswamy, V., Aminabhavi, T. M., 2011. Formulation and In Vitro Evaluation of Transdermal Delivery of Zidovudine—An Anti-HIV Drug. Journal of Applied Polymer Science. 119, 1268–1274.
26. Singh N., C.D.Upasani, 2013. Effects of penetration enhancers on *in vitro* permeability of zidovudine gels. *Indo american. J. Pharm*. Research, 3(4), 3256-3265.
27. Ongpipattanakul B., R.R.Burnette, R.O.Potts, M.L Francoeur, 1991. Evidence that oleic acid exists in a separate phase within stratum corneum lipids, Pharm. Res. 7 350–354.
28. Tanojo H., A.Bosvan Geest, J.A,Bouwstra, H.E Junginger, H.E. Bodde 1997, In vitro human skin barrier perturbation by oleic acid: thermal analysis and freeze fracture electron microscopy studies, Thermochim. Acta 293 77–85.
29. Aboofazeli R., H.Zia, T.E.Needham, 2002. Transdermal delivery of nicardipine: an approach to in vitro permeation enhancement, Drug Delivery 9, 239–247.
30. Zaslavsky B.Y., N.N.Ossipov, V.S.Krivitch, L.P.Baholdina, S.V.Rogozhin, 1978. Action of surface-active-substances on biological membranes. II. Hemolytic activity of non-ionic surfactants, Biochim. Biophys. Acta 507 1–7.
31. Yamane, M. A., A. C.Williams, B. W. Barry, 1995. Terpene penetration enhancers in propylene glycol/water co-solvent systems: effectiveness and mechanism of action. *J. Pharm. Pharmacol*. 47, 978-989.

32. El-Kattan, A. F., C. S., Asbil, B. B. Michniak, 2000. The effect of terpene enhancer lipophilicity on the percutaneous permeation of hydrocortisone formulated in HPMC gel systems. *Int. J. Pharm*. 198, 179-189.
33. Chiu, D. T., P. H. Duesberg, 1995. The toxicity of Azidothymidine (AZT) on Human and animal cells in culture at concentrations used for antiviral therapy. *Genetica*, 95, 103-109.
34. Suwanpidokkul, N.; P.Thongnopnua, K.Umprayn, 2004. Transdermal delivery of Zidovudine: the effects of vehicles, enhancers, and polymer membranes on permeation across cadaver pig skin. *AAPS Pharm. Sci. Tech* 5, 1-8.
35. Barry B.W., S.L. Bennett, 1987. Effect of penetration enhancers on the permeation of mannitol, hydrocortisone and progesterone through human skin, J. Pharm. Pharmacol. 39, 535 -546.
36. Yamane M.A., A.C.Williams, B.W. Barry, 1995. Terpene penetration enhancers in propylene glycol/water co-solvent systems: effectiveness and mechanism of action. J. Pharm. Pharmacol. 47, 978-989.
37. Narishetty S.T.K., R.Panchagnula, 2004. Transdermal delivery of Zidovudine: Effect of terpenes and their mechanism of action. J. Controlled Release. 95, 367-379.
38. Narishetty S. T. K., R.Panchagnula, 2004. Transdermal delivery system for Zidovudine: in vitro, ex vivo and in vivo evaluation. *Biopharmaceutics and drug disposition* 25, 9-20.